Communication

THE JOURNAL OF BIOLOGICAL CHEMISTRY
Vol. 270, No. 39, Issue of September 29, pp. 22693–22696, 1995

Isolation of Inactive and G Protein-resistant Adenylyl Cyclase Mutants Using Random Mutagenesis*

(Received for publication, July 21, 1995, and in revised form, August 11, 1995)

Carole A. Parent‡ and Peter N. Devreotes§

From the Department of Biological Chemistry, The Johns Hopkins University School of Medicine, Baltimore, Maryland 21205

We used random mutagenesis and phenotypic rescue of adenylyl cyclase-null *Dictyostelium* cells to isolate loss-of-function mutations in the enzyme. Mutants were (i) catalytically inactive or (ii) resistant to chemoattractant receptor and guanosine 5′-3-*O*-(thio)triphosphate stimulation. Both classes of mutants harbored substitutions within the cytoplasmic C1a domain. Mutations that inactivated the enzyme were often at highly conserved positions. Those that blocked activation were grouped in two distinct regions: one close to the plane of the plasma membrane and another halfway within the C1 loop. Missense mutations or deletions within the transmembrane domains resulted in missorting of the protein. Our screen provides a simple and efficient method to separately define the sites of catalysis and regulation of this important class of enzymes.

Adenylyl cyclases catalyze the conversion of ATP into the second messenger cAMP. Modulation of adenylyl cyclase activity by hormone and neurotransmitter receptors, through heterotrimeric guanine nucleotide-binding regulatory proteins (G proteins), underlies a wide variety of physiological events (1). The genes for eight types of mammalian, one *Drosophila*, and one *Dictyostelium* adenylyl cyclase all encode proteins that are predicted to span the membrane 12 times and contain two large cytoplasmic domains (about 40 kDa each) (2–5). Each cytoplasmic domain contains a region of homology (designated C1a and C2a) with the catalytic domains of several adenylyl and guanylyl cyclases (2, 3). Deletion analysis and site-directed mutagenesis have shown that the interaction between the two halves of the enzyme is necessary for activity and suggested that the two homologous cytoplasmic domains are not equivalent (6, 7).[1]

The receptor and G protein regulation of the adenylyl cyclase (ACA)[2] in *Dictyostelium* is analogous to that in mammalian cells (8, 9). The chemoattractant receptor, cAR1, mediates, in addition to the events involved in chemotaxis, the activation of ACA and synthesis of cAMP. The regulation of ACA is similar to mammalian type II and IV adenylyl cyclases, which are synergistically stimulated by G protein $\beta\gamma$-subunits and activated by $G_s\alpha$ (10). Indeed, genetic and biochemical analyses have established that receptor and GTPγS activation of ACA requires two components: the $\beta\gamma$-subunits of the heterotrimeric G protein G2 and a novel cytosolic protein named CRAC for cytosolic regulator of adenylyl cyclase (11, 12).

Proper regulation of ACA is essential for the early stages of development during which 10^5 cells spontaneously aggregate and differentiate into fruiting bodies. Secretion of cAMP serves to relay chemotactic signals to distal cells which, in turn, migrate toward the center to form aggregates. Consequently, *aca*$^-$, *g*β^-, and *crac*$^-$ cells cannot carry out aggregation and remain as smooth monolayers when plated on non-nutrient agar (5, 11, 12). In this study we used complementation of the *aca*$^-$ phenotype as a convenient and efficient readout to identify loss-of-function mutations in ACA.

EXPERIMENTAL PROCEDURES

Mutagenesis, Library Construction, and Transformation into aca$^-$ *Cells*—The ACA cDNA was isolated using ACA-specific probes to screen a λgt11 cDNA library made from aggregation-competent *Dictyostelium* cells (5, 13). Random mutagenesis of the ACA cDNA was performed using PCR under conditions that make the polymerase prone to misincorporations (14, 15). Specific primers containing *Nde*I (at position 799 of the ACA gene) or *Bbs*I (at position 2462) sites were used under the following conditions: 1 mM each dNTPs for weak mutagenesis and 0.5 mM dATP and 1 mM each of dCTP, dGTP, and dTTP for strong mutagenesis; 6 mM $MgCl_2$, 0.5 mM $MnCl_2$; 10 mM Tris-HCl, pH 8.3, 50 mM KCl, 0.01% gelatin, and 5 units of Taq DNA polymerase (Perkin-Elmer) for 100-μl reactions. Following an initial melting of 3 min at 94 °C, 30 cycles of denaturation (90 s at 94 °C), annealing (90 s at 55 °C), and extension (120 s at 72 °C) were performed. The PCR products were isolated and subcloned into the *Nde*I/*Bbs*I sites of a wild-type ACA cDNA in pBC (chloramphenicol-resistant) using XL-1 Blue electrocompetent cells (Stratagene). The libraries were finally transferred to an extrachromosomal *Dictyostelium* expression vector (pCP33) using the same electrocompetent bacteria. Both of these cloning steps routinely yielded greater than 50,000 independent clones. The libraries were electroporated into *aca*$^-$ cells (5) using a Bio-Rad gene pulser as described previously (16). The anticipated 4000–5000 transformants were equally divided on 24-well plates and selected using 20 μg/ml G418.

Phenotypic Screening—Screening for loss-of-function mutants was performed by clonally spreading transformants on *Klebsiella aerogenes* lawns as described (17). Single cells deposited on a bacterial lawn divide and form a plaque as the growing edge consumes the bacteria. Cells within the plaque starve and undergo development making phenotypic scoring unequivocal. About 500 transformants/well were screened by clonally spreading 100–200 clones/100-mm dish. After 4–5 days, the aggregation-deficient mutants were transferred from the plaque to liquid medium and grown under G418 selection. The selected clones were rescreened for phenotype using development on non-nutrient agar plates at 22 °C as described previously (18).

Immunoblotting—Cell samples were solubilized in Laemmli buffer (19), and 2×10^6 cell eq were subjected to 8% SDS-polyacrylamide gel electrophoresis. Immunoblotting was performed on nitrocellulose membranes using a peptide antibody directed against the last 15 amino acids of ACA. The antiserum was diluted 1:8000, and detection was performed by chemiluminescence using a donkey anti-rabbit horseradish peroxidase-coupled antibody as described by the manufacturer (Amersham Corp.).

* This work was supported by American Cancer Society Grant DB-1c. The costs of publication of this article were defrayed in part by the payment of page charges. This article must therefore be hereby marked "*advertisement*" in accordance with 18 U.S.C. Section 1734 solely to indicate this fact.

‡ Recipient of a fellowship from the Medical Research Council of Canada.

§ To whom all correspondence should be addressed: Dept. of Biological Chemistry, The Johns Hopkins University School of Medicine, 725 North Wolfe St., Baltimore MD 21205. Tel.: 410-955-4699; Fax: 410-955-5759.

[1] A. G. Gilman, personal communication.

[2] The abbreviations used are: ACA, adenylyl cyclase expressed during aggregation; GTPγS, guanosine 5′-3-*O*-(thio)triphosphate; PCR, polymerase chain reaction; WT, wild type.

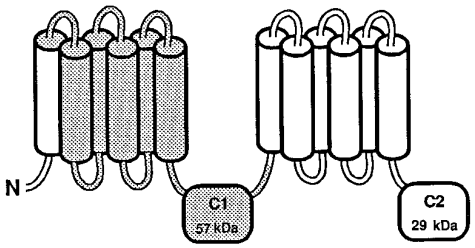

FIG. 1. **Random mutagenesis of the ACA gene.** Model of adenylyl cyclase depicting the mutagenized region (*shaded area*).

Adenylyl Cyclase Assays—Using either vegetative cells or 5-h stage cells repeatedly stimulated with 50 nM cAMP, adenylyl cyclase assays were performed as described previously with 100 μM ATP, 2 mM $MgSO_4$ (basal), 5 mM $MnSO_4$, or 40 μM GTPγS and 1 μM cAMP for 2 min at room temperature (20). For CRAC supplementation, cells were lysed into cytosol derived from cells overexpressing CRAC (21). Typically, 540 μl of cell lysates with or without GTPγS and cAMP were mixed with 120 μl of CRAC-containing supernatants and incubated on ice for 4 min, and 200 μl of this mixture was assayed. For the cAMP stimulation of adenylyl cyclase assays, 5-h stage cells were treated with 10 μM cAMP (at room temperature), lysed at the times indicated, and assayed for 1 min in the presence of exogenous CRAC (20, 21).

GTP Inhibition of cAMP Binding to cAR1—[^{3}H]cAMP binding was performed as described on membranes derived from 5-h starved cells pulsed with 50 nM cAMP in the presence or absence of 100 μM GTP (22). Bound [^{3}H]cAMP was recovered by spinning through silicone oil as described (22).

Plasmid Recovery, Phenotype Recapitulation, and Sequence Analysis—Total *Dictyostelium* DNA from 4×10^7 cells was prepared as described previously (23) and transformed into competent XL-1 Blue bacteria (Stratagene). Rescued plasmids were grown, and DNA was extracted using standard molecular biology techniques. The recovered plasmids were then transformed into *Dictyostelium aca*$^-$ cells and sequenced using Sequenase (U. S. Biochemical Corp.).

RESULTS AND DISCUSSION

Random mutagenesis of the ACA gene was achieved by error-prone PCR. We mutagenized a 1.7-kilobase pair region of the ACA cDNA corresponding to five predicted transmembrane helices as well as the C1 domain (Fig. 1). The mutagenized cDNAs were subcloned into an extrachromosomal expression vector. We used a *Dictyostelium*-specific shuttle vector (pCP33), which was shown to give high transformation efficiencies ($>10^{-4}$) and 100% segregation (*i.e.* after transformation, each transformant contains a unique mutated plasmid). pCP33 was derived from the p155d1 plasmid constructed by Hughes *et al.* (24). It contains sequences needed for extrachromosomal replication derived from *Dictyostelium* nuclear plasmid Ddp1, the neomycin gene, and a bacterial backbone for replication in *Escherichia coli*. The ACA gene was cloned downstream of the actin-15 promoter (25), which causes the ACA gene to be overexpressed compared with wild type (data not shown). The library was electroporated into *aca*$^-$ cells, and the resulting transformants were screened by clonally spreading them on *K. aerogenes* lawns (see "Experimental Procedures"). Wild-type ACA transformants aggregate to form "rough" plaques with 100% efficiency; loss-of-function mutants that fail to aggregate are readily detected as "smooth" plaques (Fig. 2*A*).

Strong and weak PCR mutagenesis conditions were used, and the results of the screens are presented in Table I. A total of 120 aggregation-deficient transformants were analyzed for ACA expression using a C-terminal peptide antibody that specifically labels a ~160-kDa band in cells overexpressing a WT ACA gene (Fig. 2*B*). Forty mutants showed protein expression. The level of expression varied between mutants and was always greater (up to 10-fold) or equal to that observed in wild-type parental cells (AX3). Upon rescreening for development on non-nutrient agar, the 40 protein-expressing mutants all remained aggregation-deficient. The non-regulated adenylyl cyclase activity of these clones was measured in the presence of $MnSO_4$ and revealed that 17 of the 40 mutants had activity (Table I). Eight mutants (4 active, 4 inactive) were selected at random and their mutated plasmid was recovered and retransformed into *aca*$^-$ cells. Each plasmid recapitulated the phenotype. Seven of the eight recapitulated mutants showed high protein expression and were either catalytically inactive (I1, I2, I3, I4) or active (U1, U2, U3) (Fig. 3, *A* and *B*). One mutant (U4) showed no protein expression upon retransformation and was discarded. Comparison of the enzymatic activities in lysates prepared from AX3 cells and from *aca*$^-$ cells overexpressing wild-type ACA (Fig. 3*B*) shows that aggregation can occur over a 10-fold range of adenylyl cyclase activity. Clearly, U1, U2, and U3 fall within this limit. Presumably, these active mutants are aggregation-deficient because they are "uncoupled" from surface receptor or G protein stimulation.

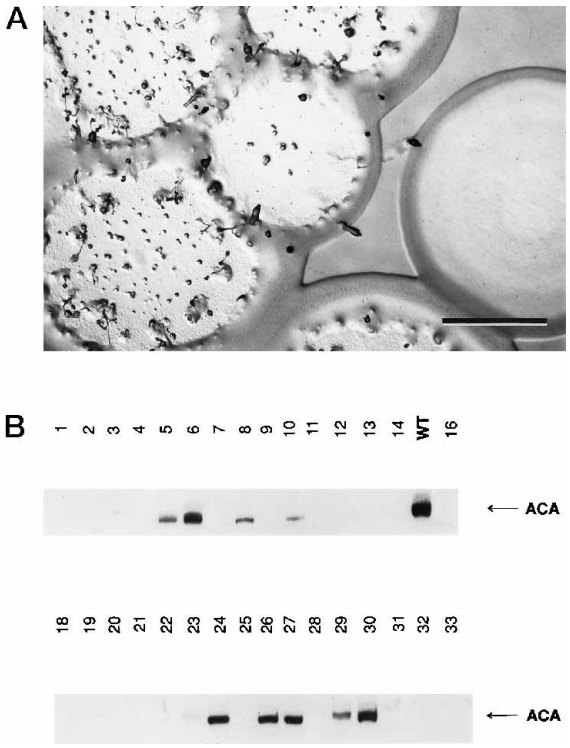

FIG. 2. **Phenotypic screen and protein expression of ACA mutants.** *A*, representative phenotypic screen; the cells were mixed with *K. aerogenes* and plated on SM agar plates. This picture, taken 5 days after plating, shows one mutant and five wild-type plaques. *Bar* represents 0.5 cm. *B*, Western analysis of selected aggregation-deficient mutants using a peptide antibody directed against the C terminus of ACA. Detection was performed using enhanced chemiluminescence. WT refers to *aca*$^-$ cells in which the wild-type ACA gene is overexpressed.

To characterize the biochemical defect in U1, U2, and U3, we dissected the receptor-G protein-adenylyl cyclase cascade. To determine if receptor-mediated activation of adenylyl cyclase was normal, we measured ACA activity, in the presence of CRAC, following the addition of exogenous cAMP to intact cells (see below) (Fig. 3*C*). Under such conditions, cells overexpressing wild-type ACA show a rapid increase in enzyme activity, peaking 1–2 min after addition of cAMP, followed by a return to basal levels within 7–10 min. Neither U1, U2, nor U3 showed chemoattractant-mediated activation of adenylyl cyclase, explaining why they fail to aggregate. To assess the integrity of the interaction between cAR1 and G2, we performed an *in vitro* GTP-induced inhibition of binding assay. In this assay, the presence of GTP, which promotes the uncoupling of the G protein α-subunit form both the receptor and its β- and γ-subunits, considerably reduces the affinity of the agonist-receptor

TABLE I
Phenotypic screen of adenylyl cyclase mutants

Mutagenesis conditions	No. of clones screened	No. of clones *agg*$^-$	Protein expression	No. of clones active (U)	No. of clones inactive (I)	Clones selected for DNA sequencing
Weak	3706	384	18/48[a]	9	9	I1, I2, U1, U2
Strong	2910	2509	22/72[a]	8	14	I3, I4, U3, U4

[a] Numerator represents number of clones expressing ACA and denominator represents total number of clones analyzed.

interaction. All three mutants showed normal high affinity binding to cAMP. In addition, in the presence of GTP, binding was reduced by 68, 65, 67, and 69% for WT, U1, U2, and U3, respectively (data not shown). Since these results showed that the defects in these mutants are downstream of G protein activation, we performed an *in vitro* GTPγS stimulation assay. As shown in Fig. 3*D*, U1, U2, and U3 exhibited no G protein-mediated activation of adenylyl cyclase. Moreover, these defects were not reversed by the addition of excess exogenous CRAC (Fig. 3*D*). Due to the limited availability of CRAC in lysates of cells overexpressing wild-type ACA, this addition typically potentiates GTPγS stimulation.

We sequenced the mutagenized inserts, and the results are summarized in Fig. 4. The overall frequency of mutagenesis was very low, even under strong PCR mutagenesis conditions, and ranged from 1 to 8 base pair changes/mutant sequenced. Of a total of 23 point mutations identified, 6 were transversions. Twenty of the 23 mutations resulted in a change of amino acid and 3 were silent. Interestingly, we also isolated a mutant bearing an in-frame 213-nucleotide (71-amino acid) deletion within the second and third transmembrane domain (U1). Out of the 20 missense point mutations characterized, only two occurred within the predicted transmembrane domains (I2, I3).

For the catalytically inactive mutants, we discovered that point mutations clustered within a highly conserved stretch of glycine residues located between positions 626 and 672 for three of the four mutants analyzed (Fig. 4*B*). Indeed, I1 displayed a single point mutation at a highly conserved glycine residue (G629C) (Fig. 4*A*). For I2 the introduction of a hydroxyl group on a neighboring conserved glycine residue (G633S) as well as an asparagine to aspartate change at position 333 also rendered the protein inactive. In addition, among its six substitutions, mutant I3 carried an isoleucine to asparagine (position 640) change at a conserved hydrophobic residue flanking one of the highly conserved glycine residues (Fig. 4*B*). These results suggest that this stretch of conserved residues within the C1a domain of ACA is important for catalytic activity. Mutant I4 exhibited six missense mutations located throughout the C1 domain (Fig. 4*A*). Interestingly, one of them (D488G) corresponded to a site-directed mutant of a highly conserved aspartate residue (D354A) shown to render the mammalian type I adenylyl cyclase catalytically inactive while still capable of binding to $G_s\alpha$.[1]

Two of the three GTPγS-insensitive mutants, U2 and U3, displayed two and three point mutations, respectively, within the C1a domain (Fig. 4*A*). Tang and Gilman (26) showed that a soluble type I/type II chimera lacking transmembrane domains retains sensitivity to $G_s\alpha$ stimulation. Our results also suggest that regulatory sites lie within the cytoplasmic domains, along with the catalytic sites. Analysis of their location revealed that the substitutions grouped in two distinct regions: one close to the plane of the plasma membrane and another halfway within the C1 loop. The cluster close to the membrane is intriguing in that regions of cytoplasmic loops abutting the fifth, sixth, and seventh transmembrane domains of surface receptors are critical for G protein interaction (27). Our data suggest that similar membrane-apposed regions are involved in G protein regulation of adenylyl cyclases. We are currently separating the two groups of mutations in U2 and U3 and isolating additional mutants to more precisely define this regulatory domain. Our results are different but not mutually exclusive from those of Chen *et al.* (28), who, using mammalian type II adenylyl cyclase peptides, recently demonstrated that Gβγ-subunits may interact with a region of C2a.

Although U1 had similar biochemical properties as U2 and

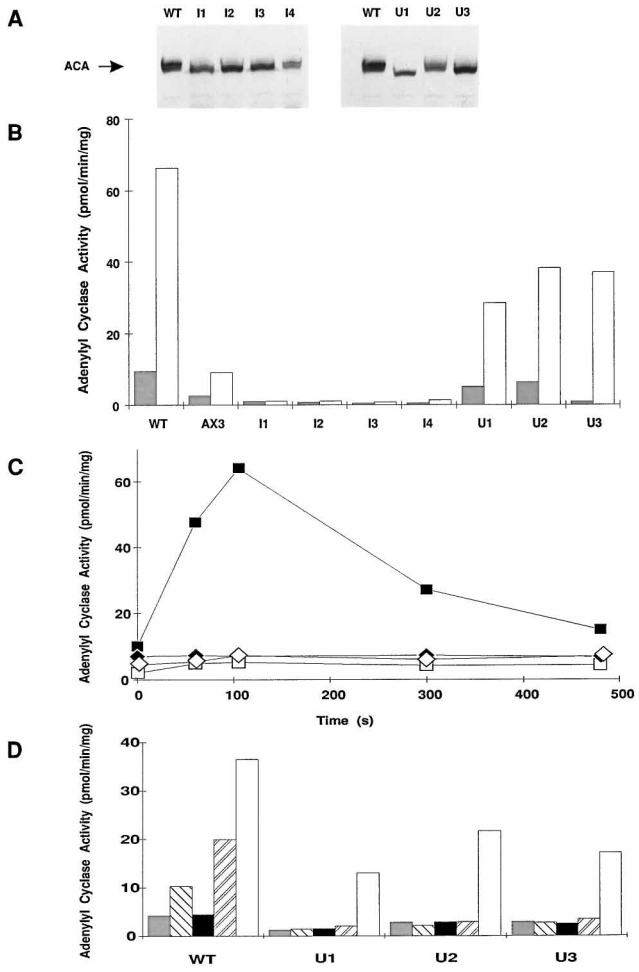

FIG. 3. **Biochemical analysis of selected ACA mutants.** The plasmids from mutants I1–I4 and U1–U3 were transformed into *aca*$^-$ cells. The resulting transformants were compared with the *aca*$^-$ cell line overexpressing the wild-type plasmid. *A*, ACA protein expression detected as in Fig. 2. *B*, basal and $MnSO_4$-stimulated adenylyl cyclase activity. The enzymatic activity of the AX3 cells (parental cell line of *aca*$^-$ cells) is shown as a control for normal expressing levels of ACA. *Gray* and *white bars* represent basal and unregulated ($MnSO_4$) conditions respectively. *C*, adenylyl cyclase activity following cAMP stimulation of catalytically active mutants. *Filled squares*, WT; *squares*, U1; *filled diamonds*, U2; *diamonds*, U3. *D*, GTPγS-stimulated adenylyl cyclase activity of U1–U3. *Gray* and *single hatched bars* represent basal and GTPγS conditions. *Black* and *double hatched bars* represent basal and GTPγS stimulation in the presence of CRAC. *White bars* represent unregulated activity ($MnSO_4$). The lower levels of ACA activity reported here, compared with previously published results, are due to the lower substrate concentration used. The results presented are representative of at least two independent experiments.

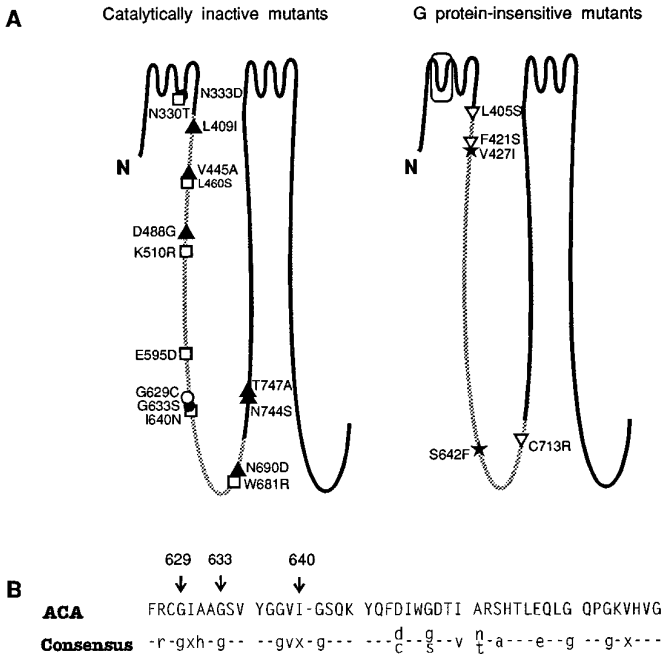

FIG. 4. **Sequence analysis of ACA mutants.** *A*, topological scheme depicting point mutations of catalytically inactive and G protein-insensitive mutants. The *gray line* depicts the conserved C1a domain. *Circle*, I1 (G629C); *filled circle*, I2 (N333D, G633S); *square*, I3 (N330T, L460S, K510R, E595D, I640N, W681R); *filled triangle*, I4 (L409I, V445A, D488G, N690D, N744S, T747A); *boxed area*, U1 (deletion 237–308); *filled star*, U2 (V427I, S642F); *inverted triangle*, U3 (L405S, F421S, C713R). *B*, amino acid sequence of ACA within the C1a loop (positions 626–672). The mutated G629 (I1), G633 (I2), and I640 (I3) residues are marked with an *arrow*. Alignment of the presumed catalytic domains of adenylyl and guanylyl cyclases from bacteria (adenylyl cyclase from *Brevibacterium liquefaciens*), sea urchin (*Strongylocentrotus purpuratus* membrane-bound guanylyl cyclase), yeast (adenylyl cyclase from *Saccharomyces cerevisiae* and *Schizosaccharomyces pompe*), *Dictyostelium* (aggregation (C1a domain) and germination specific adenylyl cyclases), trypanosome (*Trypanosoma brucei* expression site-associated gene), *Drosophila* (adenylyl cyclase, C1a domain), and mammalian (Type I–V adenylyl cyclases, C1a domain, soluble and membrane-bound guanylyl cyclases) species was obtained from W. J. Tang and A. G. Gilman. Residues that are identical in at least 75% of these sequences were included in the design of the consensus sequence shown. *x* refers to hydrophobic residues.

U3, it displayed a 71-amino acid deletion within the second and third transmembrane domain (Fig. 4*A*). Thus it would be predicted to contain only four transmembrane domains in its N-terminal half. Since this mutant showed normal catalytic activity, we were confident that it acquired an appropriate conformation. However, we reasoned that U1 might not be targeted to the correct subcellular location; missorting could preclude its appropriate receptor and G protein regulation. Xiao and Devreotes[3] recently demonstrated that cAR1 and ACA co-localize within specific plasma membrane subdomains. We carried out their subcellular fractionation procedure as an additional assessment of all the mutants. While both U2 and U3 exhibited a normal ACA distribution, U1 showed a drastically lower amount of ACA associated with cAR1 (data not shown). We propose that U1 is resistant to receptor and GTPγS stimulation mainly because it cannot access activated Gβγ-subunits. Indeed, following cAMP activation of wild-type cells, CRAC is translocated to membranes. In $g\beta^-$ cells this CRAC membrane association does not occur and GTPγS-stimulated adenylyl cyclase activation cannot be measured (21).

The catalytically inactive mutants I2 and I3 also exhibited abnormal subcellular distributions (data not shown). However, U1 illustrates that while co-localization with cAR1 may be required for appropriate regulation, it is not essential for catalytic activity. We conclude that the defects in I2 and I3 are most likely due to the mutations in C1a as described above. Interestingly, these two missorted mutants also harbored mutations within the predicted transmembrane domains (as did U1; Fig. 4*A*). These results suggest that correct sorting may be dependent on features within the transmembrane domains.

Using our screen, both catalytically inactive and receptor/G protein-resistant adenylyl cyclase mutants can be efficiently and simply isolated from a randomly mutagenized population of molecules. Indeed, this is the first report of independent mutations that clearly separate these defects. Moreover, we have devised a way to isolate gain-of-function adenylyl cyclase proteins by transforming the mutagenized ACA libraries into $crac^-$ cells and isolating aggregation-competent clones. We can use suppression of the $crac^-$ phenotype to screen for ACA mutants with high, unregulated activity or for those that retain regulated activity in the absence of CRAC, bringing more insight into the Gβγ-subunit regulation of adenylyl cyclases.

Acknowledgments—We thank Dr. Dennis Welker for supplying the p155d1 plasmid, Zhan Xiao for providing the procedure for isolation of cAR1- and ACA-containing membranes using sucrose gradients, Calin Vasiliu for sequencing, Ji Yun Kim and Michael Caterina for advice on the GTP-induced inhibition of cAMP binding, Dr. Robert Insall for helpful discussions, and Drs. Pierre Coulombe, Brenda Blacklock, and Jacqueline Milne for critical reading of the manuscript.

[3] Z. Xiao and P. N. Devreotes, manuscript in preparation.

REFERENCES

1. Gilman, A. G. (1987) *Annu. Rev. Biochem.* **56,** 615–649
2. Tang, W. J., and Gilman, A. G. (1992) *Cell* **70,** 869–872
3. Iyengar, R. (1993) *FASEB J.* **7,** 768–775
4. Krupinski, J., Lehman, T. C., Frankenfield, C. D., Zwaagstra, J. C., and Watson, P. A. (1992) *J. Biol. Chem.* **267,** 24858–24862
5. Pitt, G. S., Milona, N., Bordeis, J., Lin, K. C., Reed, R. R., and Devreotes, P. N. (1992) *Cell* **69,** 305–315
6. Tang, W. J., Krupinski, J., and Gilman, A. G. (1991) *J. Biol. Chem.* **266,** 8595–8603
7. Taissig, R., Tang, W. J., Hepler, J. R., and Gilman, A. G. (1994) *J. Biol. Chem.* **269,** 6093–6100
8. Devreotes, P. (1989) *Science* **245,** 1054–1058
9. Devreotes, P. N. (1994) *Neuron* **12,** 235–241
10. Tang, W. J., and Gilman, A. G. (1991) *Science* **254,** 1500–1503
11. Insall, R., Kuspa, A., Lilly, P. J., Shaulsky, G., Levin, L. R., Loomis, M. F., and Devreotes, P. (1994) *J. Cell Biol.* **126,** 1537–1545
12. Wu, L., Valkema, R., van Haastert, P. J. M., and Devreotes, P. N. (1995) *J. Cell Biol.* **129,** 1667–1675
13. Klein, P. S., Sun, T. J., Saxe, C. L., Kimmel, A. R., Johnson, R. L., and Devreotes, P. N. (1988) *Science* **241,** 1467–1472
14. Leung, D. W., Chen, E., and Goeddel, D. V. (1989) *Technique* **1,** 11–15
15. Cadwell, R. C., and Joyce, G. F. (1992) *PCR Methods Applications* **2,** 28–33
16. Howard, P. K., Ahern, K. G., and Firtel, R. A. (1988) *Nucleic Acids Res.* **16,** 2613–2623
17. Sussman, M. (1987) *Methods Cell Biol.* **28,** 9–29
18. Devreotes, P., Fontana, D., Klein, P., Sherring, J., and Theibert, A. (1987) *Methods Cell Biol.* **28,** 299–331
19. Laemmli, U. K. (1970) *Nature* **227,** 680–685
20. Pupillo, M., Insall, R., Pitt, G. S., and Devreotes, P. N. (1992) *Mol. Biol. Cell* **3,** 1229–1234
21. Lilly, P., and Devreotes, P. N. (1995) *J. Cell Biol.* **129,** 1659–1665
22. van Haastert, P. J. M. (1984) *Biochem. Biophys. Res. Commun.* **124,** 597–604
23. Nellen, W., Datta, S., Reymond, C., Sivertsen, A., Mann, S., Crowley, T., and Firtel, R. A. (1987) *Methods Cell Biol.* **28,** 67–100
24. Hughes, J. E., Kiyosawa, H., and Welker, D. L. (1994) *Mol. Cell. Biol.* **14,** 6117–6124
25. Knecht, D. A., Cohen, S. M., Loomis, W. F., and Lodish, H. F. (1986) *Mol. Cell. Biol.* **6,** 3973–3983
26. Tang, W. J., and Gilman, A. G. (1995) *Science* **268,** 1769–1772
27. Baldwin, J. M. (1994) *Curr. Opin. Cell Biol.* **6,** 180–190
28. Chen, J., DeVivo, M., Dinjus, J., Harry, A., Li, J., Sui, J., Carty, D. J., Blank, J. L., Exton, J. H., Stoffel, R. H., Inglese, J., Lefkowitz, R. J., Logothetis, D. E., Hildebrandt, J. D., and Iyengar, R. (1995) *Science* **268,** 1166–1169